This is an open access article published under an ACS AuthorChoice License, which permits copying and redistribution of the article or any adaptations for non-commercial purposes.

ACS APPLIED MATERIALS & INTERFACES

Research Article

www.acsami.org

Dissolution Control of Mg by Cellulose Acetate–Polyelectrolyte Membranes

Kirsi Yliniemi,*[,†] Benjamin. P. Wilson,[†,‡] Ferdinand Singer,*[,§] Sarah Höhn,[§] Eero Kontturi,[‡,⊥] and Sannakaisa Virtanen[§]

[†]Department of Chemistry, Aalto University School of Chemical Technology, P.O. Box 16100, FI-00076 AALTO, Finland

[‡]Department of Forest Products Technology, Aalto University School of Chemical Technology, P.O. Box 16300, FI-00076 AALTO, Finland

[§]Department of Materials Science and Engineering, Institute for Surface Science and Corrosion (LKO), Friedrich-Alexander-Universität Erlangen-Nürnberg, Martensstrasse 7, 91058 Erlangen, Germany

[⊥]Polymer and Composite Engineering (PaCE) group, Department of Chemical Engineering, Imperial College London, London SW7 2AZ, United Kingdom

ABSTRACT: Cellulose acetate (CA)-based membranes are used for Mg dissolution control: the permeability of the membrane is adjusted by additions of the polyelectrolyte, poly(*N*,*N*-dimethylaminoethyl methacrylate) (PDMAEMA). Spin-coated films were characterized with FT-IR, and once exposed to an aqueous solution the film distends and starts acting as a membrane which controls the flow of ions and H_2 gas. Electrochemical measurements (linear sweep voltammograms, open-circuit potential, and polarization) show that by altering the CA:PDMAEMA ratio the dissolution rate of Mg can be controlled. Such a control over Mg dissolution is crucial if Mg is to be considered as a viable, temporary biomedical implant material. Furthermore, the accumulation of corrosion products between the membrane and the sample diminishes the undesirable effects of high local pH and H_2 formation which takes place during the corrosion process.

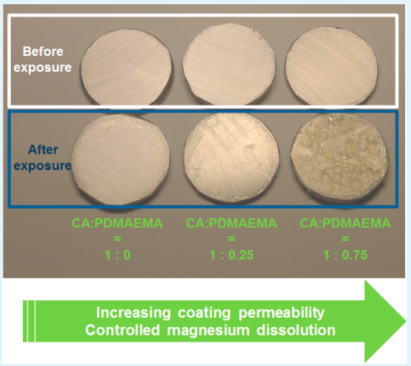

KEYWORDS: *magnesium, spin coating, controlled dissolution, implant material*

1. INTRODUCTION

Mg and Mg alloys show great potential as a temporal biomedical implant material: it dissolves easily in aqueous conditions, it is nontoxic, and its bulk properties match the properties needed from, e.g., temporal orthopedic components.[1−9] However, the rapid corrosion rates of magnesium-based materials within the physiological environment is one of the key obstacles to its wide range implementation in orthopedic components.[1−3]

When magnesium metal is subjected to ambient atmospheric conditions a sparingly soluble oxide film of magnesium hydroxide ($Mg(OH)_2$) develops that somewhat passivates the surface. However, when such a surface is placed into aqueous electrolytic physiological environments (pH 7.4−7.6) containing chloride ions, one of the most widely demonstrated interfacial reactions in chemistry occurs: the magnesium is oxidized, while the water is reduced, resulting in production of highly soluble $MgCl_2$, pH shifting hydroxide ions, and release of elementary hydrogen gas (H_2).[10,11] It is the rapidly destructive nature of these very reactions (reactions 1 and 2) in the presence of even modest levels of chloride ions (as low as 30 mM) that causes problems in many practical applications that would otherwise welcome Mg as an apt material, such as temporal implants.[9,12]

$$Mg(OH)_{2(s)} + 2Cl^-_{(aq)} \rightarrow MgCl_{2(s/aq)} + 2OH^-_{(aq)} \quad (1)$$

$$Mg_{(s)} + 2H_2O \rightarrow Mg^{2+}_{(aq)} + 2OH^-_{(aq)} + H_{2(g)} \quad (2)$$

A number of methods to overcome the high corrosion susceptibility of Mg, related H_2 evolution, and increased local pH due to formation of hydroxide ions have been proposed, ranging from protective coatings[4−8] to alloying Mg with other elements (Al, Zn, Y) and controlling the surface microstructure.[11−14] Biocompatibility and biodegradability in the coatings is advantageous in light of the many potential biomedical applications of Mg due to its physical and mechanical properties like compressive yield strength and elastic modulus being similar to those of natural bone.[9] Here, we exploited the selective membrane permeability of cellulose acetate (CA) to protect the Mg metal surface from corrosion.

The idea is that the transport of Mg^{2+}, Na^+, and Cl^- ions and H_2 gas is limited by a CA-based membrane, but the water flow takes place; thus, corrosion of Mg occurs but is diminished. In addition, blend coatings containing poly(*N*,*N*-dimethylami-

Received: September 18, 2014
Accepted: November 26, 2014
Published: November 26, 2014

 © 2014 American Chemical Society

noethyl methacrylate) (PDMAEMA) were introduced (see Scheme 1a). Selective dissolution of PDMAEMA was utilized

Scheme 1. Structural formula of (a) Poly(*N*,*N*-dimethylaminoethyl methacrylate) (PDMAEMA) and (b) Cellulose Acetate

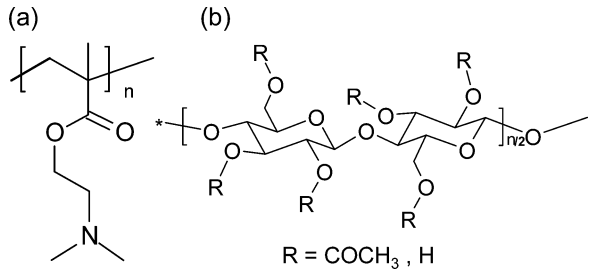

resulting in control of the membrane permeability by simply tuning the CA:PDMAEMA ratio. In general, PDMAEMA has a history of use in, e.g., antibacterial materials and gene delivery vehicles.[15−17]

CA is an acetylated derivative of cellulose which is the principal structural ingredient of all plants and the most abundant polymer in biosphere (Scheme 1b). Aside from its biobased nature and wide availability, the rationale for utilizing CA as a protective membrane stemmed from its high rejection rate for NaCl (over 90%)[18−20] and relatively low permeability of H_2 gas.[21,22] Furthermore, the rejection rate of CA membranes for Mg^{2+} ions is even higher, reportedly up to 99%, probably because of the large hydration radius of the ion.[23]

Various cellulose-based coatings have been employed for corrosion prevention of different metal surfaces in the past,[24−30] but none of these previous investigations have used CA films for dissolution control of metal, and they have not considered the semipermeable nature of CA. Control over the dissolution rate with added PDMAEMA offers an unprecedented tool for protection of Mg interfaces—something that is likely to boost the use of Mg in applications like biomedical implants.

2. EXPERIMENTAL SECTION

Both CA (50 kDa, Sigma-Aldrich) and PDMAEMA (53 kDa, Polymer Source, Inc.) were mixed in tetrahydrofuran (THF) at CA:PDMAEMA weight ratios of 1:0, 1:0.25, or 1:0.75: the amount of CA was kept constant at 50 mg/mL. A 0.25 mL amount of the solution was pipetted onto the Mg surface (99.9%, Chempur, polished up to 1200 grit using a 3:1 ethanol:glycerol mixture) or onto a SiO_2 wafer (Siltron, Inc., cleaned with UV light and ozone) and spin coated for 90 s at 1500 rpm.

Spin-coated samples were exposed to 0.1 M NaCl solution (pH adjusted with NaOH to pH = 7.4 prior to measurements), and linear sweep voltammograms (LSV, 5 mV/s) and polarization at −1.5 V vs Ag/AgCl for 90 min were measured in a three-electrode setup, with a Ag/AgCl reference electrode and Pt counter electrode. The open-circuit potential (OCP) was also recorded as a function of time using the same cell setup. OCP, polarization, and LSV measurement were all repeated using fresh samples.

After the measurements, the pH in close proximity to the sample surface was measured. In addition, two samples of the solution, one from between the membrane and the substrate and the other from the bulk solution, were obtained immediately after the polarization experiments using a hypodermic syringe with a needle. These samples were subsequently analyzed for Mg^{2+} ion concentration by ICP-OES (PerkinElmer, Optima 8300) using argon plasma (flow rate 10 l min^{-1}).

The cell setup featured an aperture that provided an exposed sample area of 3.14 cm^2. This configuration also had the additional advantage of anchoring the spin-coated CA:PDMAEMA film in place throughout the duration of the measurement: the membrane becomes distended from the Mg surface when exposed to water and as corrosion proceeds, the corrosion products are accumulated between membrane and sample (Figure 1).

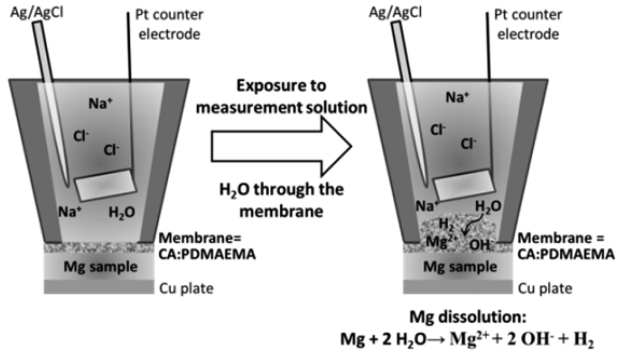

Figure 1. Experimental setup: exposure to the measurement solution (0.1 M NaCl, pH = 7.4) causes H_2O flow through the membrane and Mg dissolution starts. Corrosion products are accumulated between the membrane and the sample.

The surface morphology of the freshly spin-coated CA:PDAEMA coatings on silicon wafer, prior to immersion, was investigated by AFM using a MultiMode 8 scanning probe microscope (Bruker AXS Inc., Madison, WI). Images were acquired in air by tapping mode with a silicon cantilever (NSC15/AIBS from Ultrasharp μmasch, Tallinn, Estonia), and the typical resonance frequency of the cantilever was 325 kHz. Imaging was repeated on two replica samples with a minimum of two different surface regions characterized.

Water uptake was measured by comparing the weight of either Si wafer supported films or free-standing membranes before and after 30 min immersion in ultrapure Milli-Q water (MQ) (Millipore Corp.). The free-standing membranes were prepared by spin coating CA:PDMAEMA solutions on a silicon wafer (used to avoid complications due to possible corrosion products), exposing the samples into MQ water for a minimum of 30 min, and gently peeling off the membrane from the wafer surface. These free-standing films were dried overnight in a desiccator and weighed prior to immersion in MQ water and reweighing.

Samples were characterized after spin coating by FT-IR (Thermo Scientific, Nicolet 6700 with an ATR-D cell: 32 scans between 4000 and 500 cm^{-1}), and selective dissolution of PDMAEMA was studied after 30 min exposure to MQ water.

3. RESULTS AND DISCUSSION

The dry, spin-coated films on Si wafer were first characterized with AFM to determine the topography of the films (CA:PDMAEMA = 1:0, 1:0.25, or 1:0.75), and Figure 2 shows that addition of PDMAEMA results in clear changes to the surface features. With pure CA it is possible to discern a number of heterogeneous-sized pores within the sample area, and this is in line with the findings of Valente et al.,[31] who also studied spin-coated CA films (from THF). Addition of PDMAEMA results in a smoother surface profile with larger and deeper pore-like features.

The presence of PDMAEMA within the dry, spin-coated film before and after exposure to water was studied with FT-IR, and this is shown in Figure 3: FT-IR spectra are normalized with respect to the intensity of the band at 1736 cm^{-1}. The

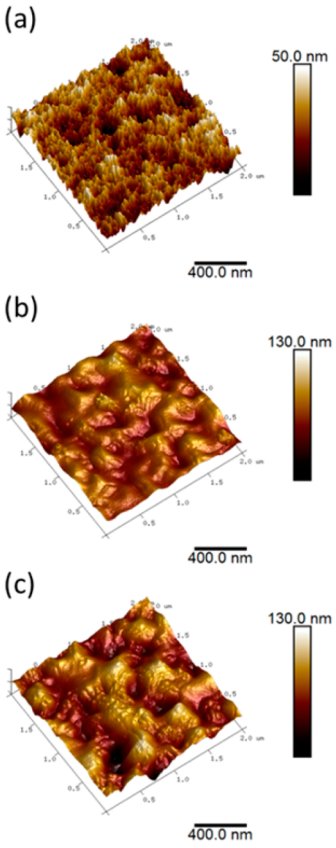

Figure 2. Topography of the spin-coated CA:PDMAEMA coatings on a silicon wafer measured by AFM: CA:PDMAEMA = (a) 1:0, (b) 1:0.25, and (c) 1:0.75. (Note the different height bars for a and b and c).

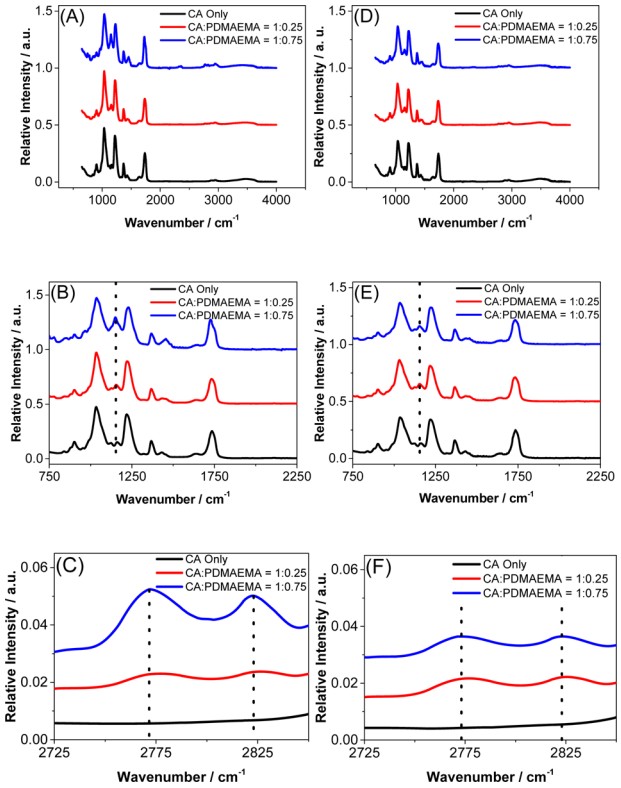

Figure 3. ATR FT-IR spectra of CA:PDMAEMA coatings on Mg before (A–C) and after (D–F) immersion in MQ water for 30 min: (A and D) full spectrum, while (B–C and E–F) magnifications at selected wavenumber ranges.

characteristic cellulose acetate bands at 902, 1031, 1222, 1369, and 1736 cm^{-1} are observed by FT-IR both before and after exposure to the MQ water (Figure 3), and these values correlate well with those found in the literature.[32]

The bands around 1100–1200 cm^{-1} are due to an amine bond (C–N stretching[33] or C–C–N bending[34]) and ester group (C–O–C bending[33]), both present in PDMAEMA. There is also a small intensity band at these wavenumbers with a pure cellulose acetate sample, as CA also has a C–O–C ester group, but as can be seen, the amine and/or ester band is more intense when PDMAEMA is present (Figure 3b). Additionally, the bands observed around 2772 and 2822 cm^{-1} can be related to C–H stretching of the $N-(CH_3)_2$ group (2776 and 2821 cm^{-1} according to Feldstein et al.;[33] 2770 and 2884 cm^{-1} according to Roy et al.[34]), present only in PDMAEMA, and there are no bands for cellulose acetate at these wavelength numbers (Figure 3 c). Using these three bands (1151, 2772, and 2822 cm^{-1}) in Figure 3 as markers for PDMAEMA, it can be seen that there is an increased amount of PDMAEMA at a ratio of 1:0.75 (CA:PDMAEMA) when compared to the ratio 1:0.25.

Additionally, after 30 min exposure to MQ water, the majority of PDMAEMA has dissolved from the surface (Figure 3d–f), and this presumably leads to a higher permeability at a ratio of 1:0.75 than at 1:0.25 or 1:0. The residual PDMAEMA within the films (which can be seen in Figure 3f) could further improve the corrosion control of the system due to its well-known pH sensitivity:[15,35] at the acidic–near neutral pH range PDMAEMA is protonated and swollen, while in the alkaline pH range it is in a collapsed form as seen, for example, in numerous hydrogel studies.[33,36,37] Mg dissolution gives rise to increased alkaline pH, resulting in the collapsed state of residual PDMAEMA that in turn would tend to block the surface and provide additional protection to the Mg substrate.

Water uptake of spin-coated films on Si wafer was also investigated by measuring the weight of the samples before and after exposure to MQ water, and it is clear that the pure CA coating absorbs clearly less water than PDMAEMA-containing films in the order 1:0 (less than 1%) < 1:0.25 (around 2%) < 1:0.75 (around 6%). However, the actual water uptake percentages must be taken into account with great care as the simultaneous dissolution of PDMAEMA, the nature of the substrate, and the water between the sample and the film causes inherent error within the measured values.

Exposure of CA:PDMAEMA film to an aqueous solution detaches it from the Mg surface, and it begins to behave like a membrane which can limit ion and gas flow. In this study the cell setup is such that the membrane stays attached to the Mg sample sides (Figure 1). An example of a distended membrane is illustrated in the photographs, taken after the sample is removed from the cell (Figure 4a and 4b); the detached dry CA membrane can be easily handled with tweezers. Figure 4c shows how the different types of coatings behave when the surface is covered with MQ water: the higher the PDMAEMA content is, the more water has penetrated through and the membrane becomes distended in those areas.

Also, water uptake was investigated for free-standing membranes, and a similar trend was observed as with silicon supported films (water uptake increasing in order 1:0 < 1:0.25

dx.doi.org/10.1021/am5063597 | ACS Appl. Mater. Interfaces 2014, 6, 22393–22399

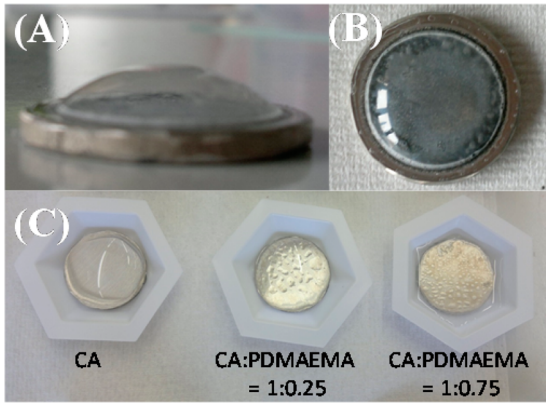

Figure 4. Photographs of CA- and CA:PDMAEMA-coated Mg samples: (a and b) CA:PDMAEMA = 1:0.75 coating after polarization to −1.5 V vs Ag/AgCl in 0.1 M NaCl for 90 min, and (c) coatings covered by MQ water (after 30 min exposure).

< 1:0.75). Due the nature of the wet, free-standing membranes, which can easily fold around themselves to trap extraneous water droplets, only a qualitative estimation of water uptake could be performed.

To study how such a membrane would control the corrosion, electrochemical measurements—linear sweep voltammograms (LSV), open-circuit potential (OCP) recording, and polarization to a value near the OCP—were performed. The results of LSV measurements (measured from fresh samples after 5, 15, and 30 min exposure to 0.1 M NaCl solution at pH = 7.4) are displayed in Figure 5.

As can be seen from Figure 5, the corrosion potential of the samples is similar in all cases, especially with a longer exposure time. This is not surprising as the membrane is not a coating in a classical sense, but rather, the bare Mg is exposed to the solution, while the role of the CA:PDMAEMA membrane is to control the flow of ions and H_2 gas and, thus, the degree of dissolution rather than the corrosion mechanisms.

The effect of PDMAEMA content in the membrane can be seen from the LSV curves: the anodic branch of LSV with a membrane ratio of 1:0.25 behaves more like the sample with the pure CA membrane, especially after 30 min, providing lower corrosion susceptibility. In contrast, the sample covered by the membrane with a ratio of 1:0.75 shows an intermediate behavior between CA coated and pure Mg.

To further investigate the corrosion behavior, the open-circuit potential (OCP) in 0.1 M NaCl was recorded as a function of time (Figure 6). As can be observed, all samples reach rather similar and constant OCP values after the first 5−10 min of exposure. In fact, the pure Mg sample reaches a stable reading around −1.5 V vs Ag/AgCl after only 5 min, whereas the coated samples are slower due to water uptake into the film and PDMAEMA dissolution.

The degree of corrosion, on the other hand, can be altered, and it was studied by recording the current density when the sample was polarized to a constant value near the OCP, i.e., −1.5 V vs Ag/AgCl, and the results are shown in Figure 7. Here, a clear difference in the current density is seen between the different samples. For pure Mg the results show a relatively high current density during the first 40 min, suggesting a high corrosion rate, while the presence of the CA membrane demonstrates an almost passive behavior throughout the whole measurement time. The behavior of CA:PDMAEMA samples displays features of both the pure Mg sample and the sample

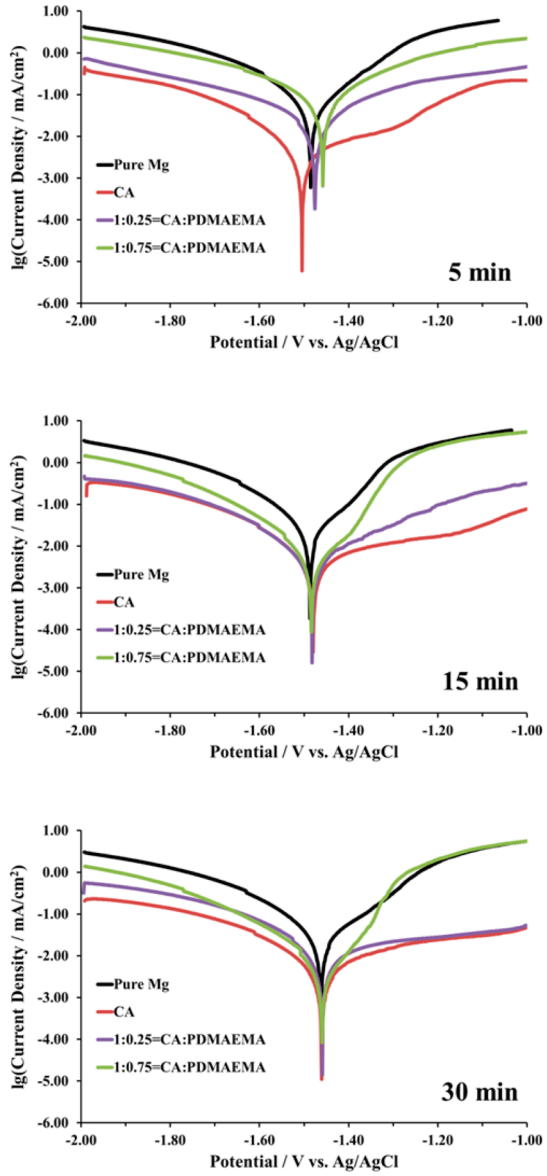

Figure 5. Linear sweep voltammetry of the samples after 5, 15, and 30 min exposure to 0.1 M NaCl solution (sweep rate 5 mV/s).

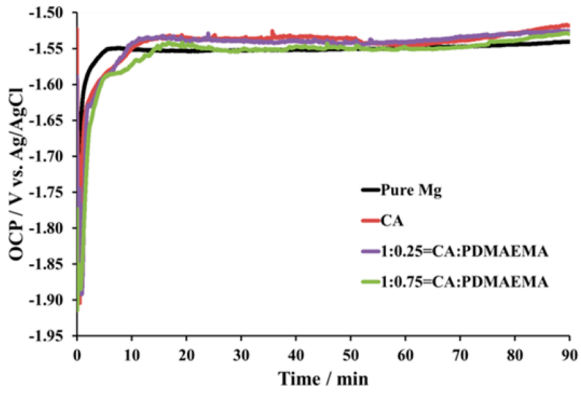

Figure 6. Open-circuit potential of samples as a function of time in 0.1 M NaCl.

with pure CA membrane as with increasing PDMAEMA content higher currents are observed only during the first 20 min after which the corrosion is reduced. The shorter time

dx.doi.org/10.1021/am5063597 | ACS Appl. Mater. Interfaces 2014, 6, 22393−22399

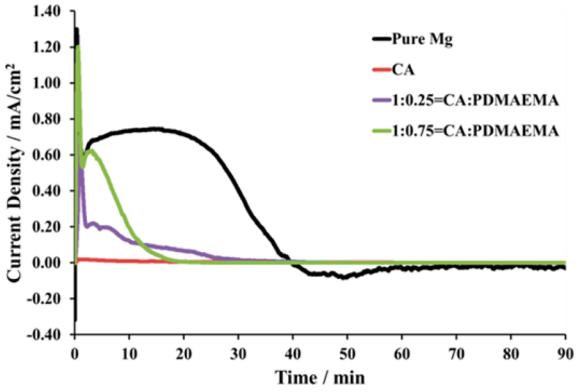

Figure 7. Polarization of the samples to −1.5 V vs Ag/AgCl in 0.1 M NaCl.

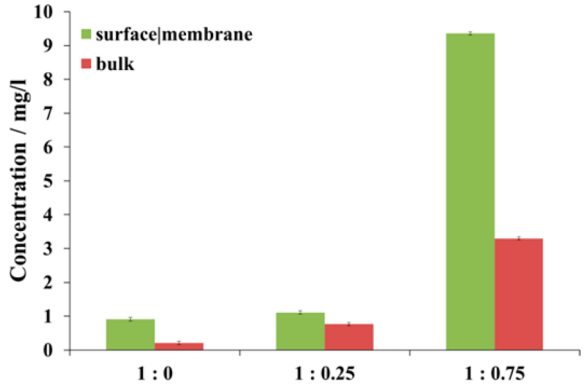

Figure 8. Concentration of Mg^{2+} ions between the surface and the membrane (surfacelmembrane) and in bulk solution (bulk) after polarization to −1.5 V vs Ag/AgCl for 90 min. The CA:PDMAEMA ratio in the membrane was 1:0, 1:0.25, or 1:0.75.

needed for a reduced corrosion with CA:PDMAEMA membrane is believed to be due to the accumulation of corrosion products between the substrate surface and the membrane: Mg dissolution increases pH due to OH^- ion formation, and pH values > 11 are known to repassivate the Mg surface as a result of formation of $MgO/Mg(OH)_2$ layers.[4,38]

From these electrochemical measurements it can be concluded that the corrosion rate is changed due to the presence of CA:PDMAEMA or CA membrane, and moreover, the PDMAEMA content can be used to control the rate of initial corrosion. This is crucial when considering the possible use as a temporal implant as one of the big challenges in the field has been the need to control the initial corrosion rate of Mg dissolution. Additionally, it is worth noting that part of the evolved H_2 gas is trapped by the CA:PDMAEMA membrane. However, the CA membrane does not create a perfect barrier for H_2, but if a balance between H_2 formation due to corrosion and H_2 flow through the membrane is found, a more stable corrosion rate can result. Thus, a semipermeable membrane on the Mg surface can be used to overcome another main obstacle in the use of Mg as a temporal implant material, namely, adverse gas flow to the surrounding tissue and bloodstream. The performance shown by the samples outlined in Figures 5−7 demonstrates the fact that the membrane controls the flow of ions and gas.

Accumulation of corrosion products, especially Mg^{2+} ions, between the membrane and the sample was studied by ICP-OES, and the results are outlined in Figure 8. Such results clearly demonstrate that Mg^{2+} ions accumulate between the surface and the membrane and also that more dissolution of Mg takes place with increasing PDMAEMA content, as was seen previously from the polarization data (Figure 7). These facts again demonstrate that PDMAEMA content does control the permeability, which in turn controls Mg dissolution.

The high increase of local pH during dissolution, which can result in tissue damage, is one of the major limitations to the use of Mg as a temporal medical implant material. In order to determine if CA-based membranes were able to ameliorate this problem, pH values were measured after both polarization and OCP experiments, and the results are detailed in Table 1.

As can be seen, the pH of the bulk solution after OCP and polarization measurements of pure Mg samples increases from 7.4 (at the start of the measurement) to 10.7 and 11.3, respectively. When the pH is measured from a sample with the CA membrane, it stayed relatively constant during the OCP and polarization measurements (6.8 and 7.1, respectively).

Table 1. Solution pH Measured in Close Proximity to the Sample after Open-Circuit Potential Measurements (90 min) or Polarization at −1.5 V vs Ag/AgCl

sample	pH after OCP	pH after polarization
pure Mg	10.7	11.3
CA Only	6.8	7.1
CA:PDMAEMA = 1:0.25	7.2	9.6
CA:PDMAEMA = 1:0.75	7.2	9.8

When the ratio of PDMAEMA was increased (1:0.25 and 1:0.75) the pH values after OCP remained constant (7.2 for both cases) and increased to a lesser extent, cf. pure Mg, during the polarization measurements (9.6 and 9.8, respectively). This further enhances the theory of accumulated corrosion products under the membrane and shows that selective dissolution of PDMAEMA leads to the control of permeability.

The CA-based membranes presented here are by no means a final solution for Mg dissolution control, and more studies and optimization are clearly needed. The main disadvantages of the system are the detachment of the membrane from the Mg surface within the first few minutes of exposure to an aqueous solution (the cell setup in the experiments presented here kept the membrane in place) and H_2 trapping between the membrane and the sample (if not optimized properly this could lead to rupture of the membrane during prolonged exposure). Therefore, if these types of membranes are to be used in real-life applications, more studies and modifications are needed.

However, when compared to classical coatings or micro-structuring of Mg surface for biomedical applications,[4−8] the approach outlined here has obvious advantages. These include an ability to protect the surrounding tissue from the initial high corrosion rate and pH increase, and it can also alleviate the problems caused by rapid H_2 evolution during corrosion. These drawbacks have long been the main obstacles in the use Mg in biomedical fields. Additionally, CA membranes are cheap and already commercially available, and recently, there has been lots of research on their biodegradability.[39]

Furthermore, the membranes outlined here can also be used in conjunction with other existing protection methods reported in the literature, e.g., coatings, conversion layers, and microstructuring, leading to multileveled dissolution control of temporal Mg based medical implants.

4. CONCLUSIONS

This study introduces, for the very first time, the use of CA-based membranes for controlling the dissolution of Mg: dissolution control is critical for the realizing the use of Mg as temporal medical implants. Dissolution control is achieved by the limited ion and H_2 flow through the membrane, and the permeability of the membrane can be adjusted by combining a cationic polyelectrolye, PDMAEMA, to the CA membrane. By altering the CA:PDMAEMA ratio, the initial corrosion rate of Mg was able to be controlled as selective dissolution (proved by FT-IR) of PDMAEMA takes place once the membrane is exposed to an aqueous solution. Electrochemical measurements show that the degree of corrosion is higher when the PDMAEMA content is increased, and ICP results enhance this conclusion.

Moreover, CA and CA:PDMAEMA membranes have the additional advantages of controlling the pH level in the surrounding environment and H_2 flow as corrosion products are accumulated between the membrane and the sample surface: when Mg is covered by the CA membrane the pH values stay close to near neutral after 90 min of exposure. In short, this study clearly demonstrates how CA-based membranes control Mg dissolution and regulate the associated undesirable pH increase.

AUTHOR INFORMATION

Corresponding Authors

*E-mail: kirsi.yliniemi@aalto.fi.
*E-mail: ben.wilson@aalto.fi.

Author Contributions

The manuscript was written through contributions of all authors. All authors have given approval to the final version of the manuscript.

Notes

The authors declare no competing financial interest.

ACKNOWLEDGMENTS

The authors acknowledge the Academy of Finland (Project Nos. 263551 (K.Y.) and 259500 (E.K.)), Aalto University's "Forest Meets Chemistry" initiative (B.W.), and the German Research Foundation, DFG, for funding this work. Also, the J. W. T. Jones Travelling Fellowship of the Royal Society of Chemistry is thanked for funding B. P. Wilson's visit to Friedrich-Alexander-Universität Erlangen-Nürnberg.

REFERENCES

(1) Witte, F.; Hort, N.; Vogt, C.; Cohen, S.; Kainer, K. U.; Willumeit, R.; Feyerabend, F. Degradable Biomaterials Based on Magnesium Corrosion. *Curr. Opin. Solid State Mater. Sci.* **2008**, *12*, 63−72.

(2) Virtanen, S. Biodegradable Mg and Mg alloys: Corrosion and Biocompatibility. *Mater. Sci. Eng., B* **2011**, *176*, 1600−1608.

(3) Zheng, Y. F.; Gu, X. N.; Witte, F. Biodegradable Metals. *Mater. Sci. Eng., R* **2014**, *77*, 1−34.

(4) Hornberger, H.; Virtanen, S.; Boccaccini, A. R. Biomedical Coatings on Magnesium Alloys. *Acta Biomater.* **2012**, *8*, 2442−2455.

(5) Shadanbaz, S.; Dias, G. J. Calcium Phosphate Coatings on Magnesium Alloys for Biomedical Applications. *Acta Biomater.* **2012**, *8*, 20−30.

(6) Wu, G.; Ibrahim, J. M.; Chu, P. K. Surface Design of Biodegradable Magnesium Alloys. *Surf. Coat. Technol.* **2013**, *233*, 2−12.

(7) Zhou, J.; Zhang, X.; Lin, Q.; Liu, Y.; Chen, F.; Li, L. Effect of the Physiological Stabilization Process on the Corrosion Behaviour and Surface Biocompatibility of AZ91D Magnesium Alloy. *J. Mater. Chem. B* **2013**, *1*, 6213−6224.

(8) Narayanan, T. S. N. S.; Park, I. S.; Lee, M. H. Tailoring the Composition of Fluoride Conversion Coatings to Achieve Better Corrosion Protection of Magnesium for Biomedical Applications. *J. Mater. Chem. B* **2014**, *2*, 3365−3382.

(9) Staiger, M. P.; Pietak, A. M.; Huadmai, J.; Dias, G. Magnesium and its Alloys as Orthopedic Biomaterials. *Biomaterials* **2006**, *27*, 1728−1734.

(10) Kirkland, N. T.; Birbilis, N.; Staiger, M. P. Assessing the corrosion of biodegradable magnesium implants: A critical review of current methodologies and their limitations. *Acta Biomater.* **2012**, *8*, 925−936.

(11) Li, N.; Zheng, Y. Novel Magnesium Alloys Developed for Biomedical Application. *J. Mater. Sci. Technol.* **2013**, *29*, 489−502.

(12) Zhang, L.-N.; Hou, Z.-T.; Ye, X.; Xu, Z.-B.; Bai, X.-L.; Shang, P. The Effect of Selected Alloying Element Additions on Properties of Mg-based Alloy as Bioimplants. *Front. Mater. Sci.* **2013**, *7*, 227−236.

(13) Hänzi, A. C.; Sologubenko, A. S.; Uggowitzer, P. J. Design Strategy for New Biodegradable Mg-Y-Zn Alloys for Medical Applications. *Int. J. Mater. Res.* **2009**, *100*, 1127−1136.

(14) Kirkland, N. T.; Staiger, M. P.; Nisbet, D.; Davies, C. H. J.; Birbilis, N. Performance-driven Design of Biocompatible Mg Alloys. *JOM* **2011**, *63*, 28−34.

(15) Hu, J.; Zhang, G.; Ge, Z.; Liu, S. Stimuli-responsive Tertiary Amine Methacrylate-based Block Copolymers: Synthesis, Supramolecular Self-assembly and Functional Applications. *Prog. Polym. Sci.* **2014**, *39*, 1096−1143.

(16) Mintzer, M. A.; Simanek, E. E. Nonviral Vectors for Gene Delivery. *Chem. Rev.* **2009**, *109*, 259−302.

(17) Agarwal, S.; Zhang, Y.; Maji, S.; Greiner, A. PDMAEMA Based Gene Delivery Materials. *Mater. Today (Oxford, U.K.)* **2012**, *15*, 388−393.

(18) Yu, S.; Cheng, Q.; Huang, C.; Liu, J.; Peng, X.; Liu, M.; Gao, C. Cellulose Acetate Hollow Fiber Nanofiltration Membrane with Improved Permselectivity Prepared Through Hydrolysis Followed by Carboxymethylation. *J. Membr. Sci.* **2013**, *434*, 44−54.

(19) Petersen, R. R. Composite Reverse Osmosis and Nanofiltration Membranes. *J. Membr. Sci.* **1993**, *83*, 81−150.

(20) Geise, G. M.; Paul, D. R.; Freeman, B. D. Fundamental Water and Salt Transport Properties of Polymeric Materials. *Prog. Polym. Sci.* **2014**, *39*, 1−42.

(21) Puleo, A. C.; Paul, D. R.; Kelley, S. S. The Effect of Degree of Acetylation on Gas Sorption and Transport Behavior in Cellulose Acetate. *J. Membr. Sci.* **1989**, *47*, 301−332.

(22) Basu, S.; Khan, A. L.; Cano-Odena, A.; Liu, C.; Vankelecom, I. F. J. Membrane-based Technologies for Biogas Separations. *Chem. Soc. Rev.* **2010**, *39*, 750−768.

(23) Reid, C. E.; Breton, E. J. Water and Ion Flow Across Cellulosic Membranes. *J. Appl. Polym. Sci.* **1959**, *1*, 133−143.

(24) Yabuki, A.; Kawashima, A.; Fathona, I. W. Self-Healing Polymer Coatings with Cellulose Nanofibers Served as Pathways for the Release of a Corrosion Inhibitor. *Corros. Sci.* **2014**, *85*, 141−146.

(25) Tamborim, S. M.; Dias, S. L. P.; Silva, S. N.; Dick, L. F. P.; Azambuja, D. S. Preparation and Electrochemical Characterization of Amoxicillin-doped Cellulose Acetate Films for AA2024-T3 Aluminum Alloy Coatings. *Corros. Sci.* **2011**, *53*, 1571−1580.

(26) Norouzia, M.; Garekania, A. A. Corrosion Protection by Zirconia-based Thin Films Deposited by a Sol−Gel Spin Coating Method. *Ceram. Int.* **2014**, *40*, 2857−5861.

(27) Chen, Q.; Pérez de Larraya, U.; Garmendia, N.; Lasheras-Zubiate, M.; Cordero-Ariasa, L.; Virtanen, S.; Boccaccinia, A. R. Electrophoretic Deposition of Cellulose Nanocrystals (CNs) and CNs/Alginate Nanocomposite Coatings and Free Standing Membranes. *Colloids Surf., B* **2014**, *118*, 41−48.

(28) Ritter, J. J.; Rodriguez, M. J. Corrosion Phenomena for Iron Covered with a Cellulose Nitrate Coating. *Corrosion* **1982**, *38*, 223−226.

(29) Umoren, S. A.; Solomon, M. M.; Udosoro, I. I.; Udoh, A. P. Synergistic and Antagonistic Effects Between Halide Ions and Carboxymethyl Cellulose for the Corrosion Inhibition of Mild Steel in Sulphuric Acid Solution. *Cellulose* **2010**, *17*, 635−648.
(30) Solomon, M. M.; Umoren, S. A.; Udosoro, I. I.; Udoh, A. P. Inhibitive and Adsorption Behaviour of Carboxymethyl Cellulose on Mild Steel Corrosion in Sulphuric Acid Solution. *Corros. Sci.* **2010**, *52*, 1317−1325.
(31) Valente, A. J.M.; Ya. Polishchuk, A.; Burrows, H. D.; Lobo, V. M. M. Permeation of water as a tool for characterizing the effect of solvent, film thickness and water solubility in cellulose acetate membranes. *Eur. Polym. J.* **2005**, *41*, 275−281.
(32) Pouchert, C. J. *The Aldrich Library of FT-IR Spectra*, 1st ed.; Aldrich Chemical Co.: Milwaukee, WI, 1985; Vol. 2.
(33) Feldstein, M. M.; Kiseleva, T. I.; Bondarenko, G. N.; Kostina, J. V.; Singh, P.; Cleary, G. W. Mechanisms of Molecular Interactions in Polybase−Polyacid Complex Formed by Copolymers of N,N-dimethylaminoethyl methacrylate with Alkylmethacrylates and Methacrylic Acid with Ethylacrylate. *J. Appl. Polym. Sci.* **2009**, *112*, 1142−1165.
(34) Roy, D.; Knapp, J. S.; Guthrie, J. T.; Perrier, S. Antibacterial Cellulose Fiber via RAFT Surface Graft Polymerization. *Biomacromolecules* **2008**, *9*, 91−99.
(35) Orakdogen, N. pH-responsive Swelling Behavior, Elasticity and Molecular Characteristics of Poly(N,N dimethylaminoethyl methacrylate) Gels at Various Initial Monomer Concentrations. *Polym. Bull.* **2011**, *67*, 1347−1366.
(36) Şen, M.; Aguş, O.; Safrany, A. Controlling of Pore Size and Distribution of PDMAEMA Hydrogels Prepared by Gamma rays. *Radiat. Phys. Chem.* **2007**, *76*, 1342−1346.
(37) Wang, Z.-C.; Xu, X.-D.; Chen, C.-S.; Wang, G.-R.; Wang, B.; Zhang, X.-Z.; Zhuo, R.-X. Study on Novel Hydrogels Based on Thermosensitive PNIPAAm with pH Sensitive PDMAEMA Grafts. *Colloids Surf., B* **2008**, *67*, 245−252.
(38) Pourbaix, M. *Atlas of Electrochemical Equilibrium in Aqueous Solutions*; Pergamon Press: Oxford, 1966.
(39) Puls, J.; Wilson, S. A.; Ölter, D. Degradation of Cellulose Acetate-based Materials. *J. Polym. Environ.* **2011**, *19*, 152−165.